

Supplementary Information

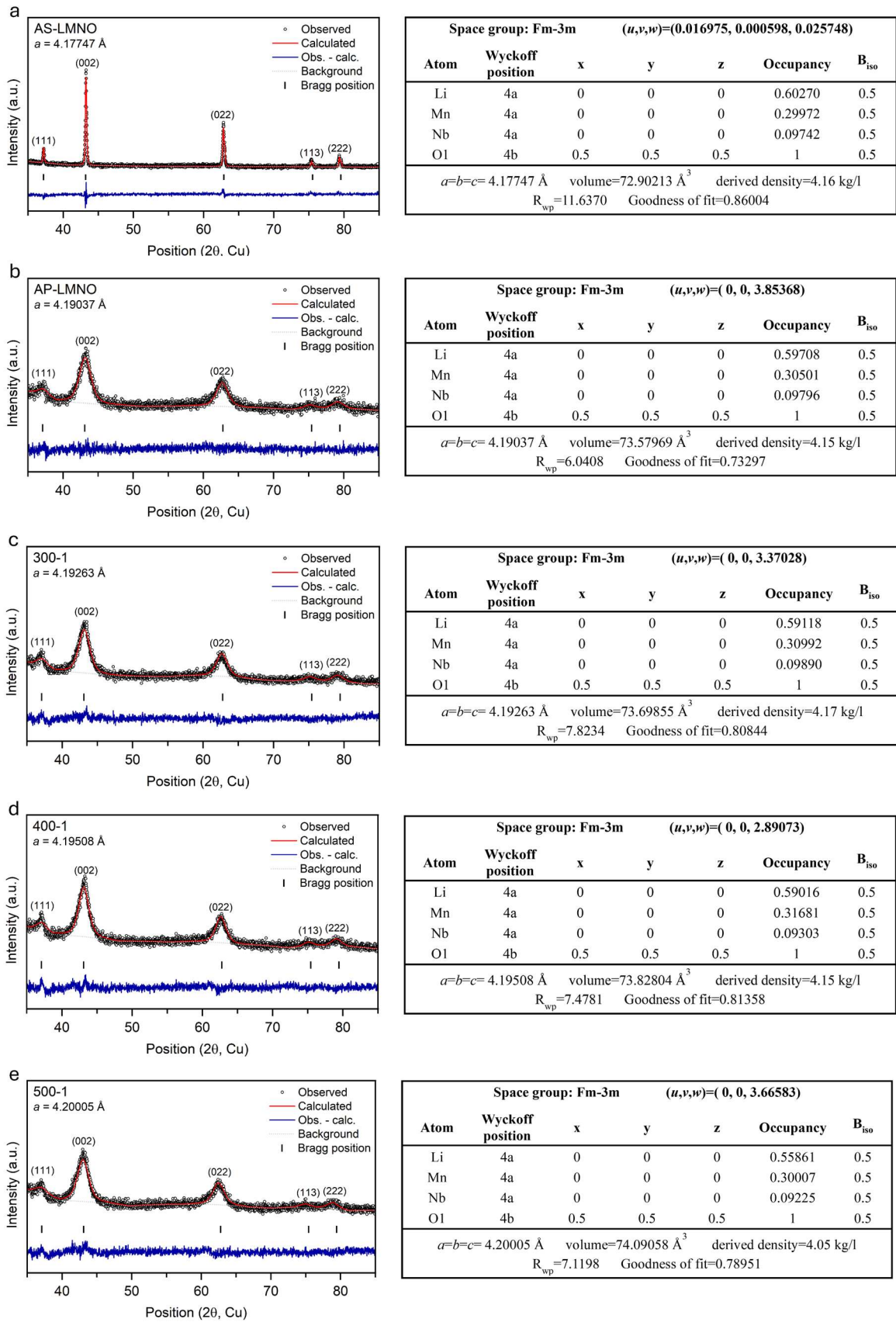
Mitigating Carbothermal Reduction in Disordered Rock-Salt Cathodes via Direct Electrode-Slurry Carbon Mixing

Gregory Lazaris,^{1‡} Yixuan Zhang,^{1‡} Pablo Trevino Lara,¹ Nicolas Brodusch,¹ Raynald Gauvin¹ and Jinhyuk Lee^{1*}

¹ Department of Mining and Materials Engineering, McGill University, Montréal, QC H3A 0C5, Canada

‡ These authors contributed equally to this work.

* Correspondence and requests for materials should be addressed to Jinhyuk Lee (jinhyuk.lee@mcgill.ca)



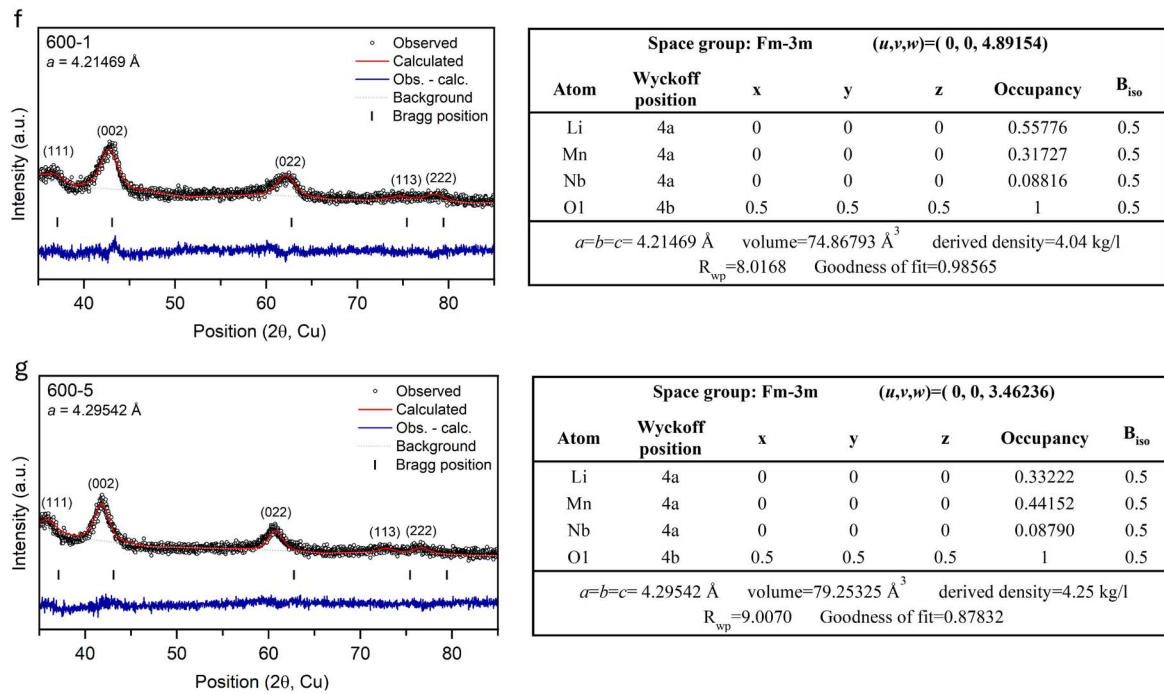


Figure S1. XRD refinement data for (a) AS-LMNO, (b) AP-LMNO, (c) 300-1, (d) 400-1, (e) 500-1, (f) 600-1 and (g) 600-5. XRD refinements and structural parameters were obtained as follows: The crystallographic structure of LiFeO₂ (ICSD collection code 51208) in the Fm $\bar{3}$ m space group served as the reference input file, and a Pseudo-Voigt profile function was employed. Initially, lattice parameters were refined using atomic fractions based on the chemical composition of Li_{1.2}Mn_{0.6}Nb_{0.2}O₂ as the starting atomic occupancies. Subsequently, both lattice parameters and cation atomic occupancies were refined simultaneously. The same procedure was applied to all XRD refinements provided in the Supplementary Information.

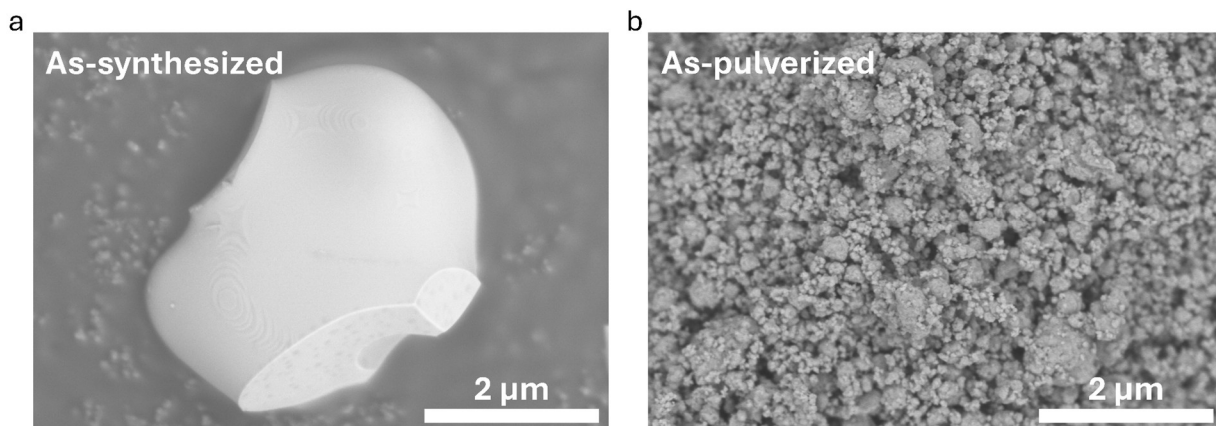


Figure S2. SEM images of (a) as-synthesized and (b) as-pulverized LMNO.

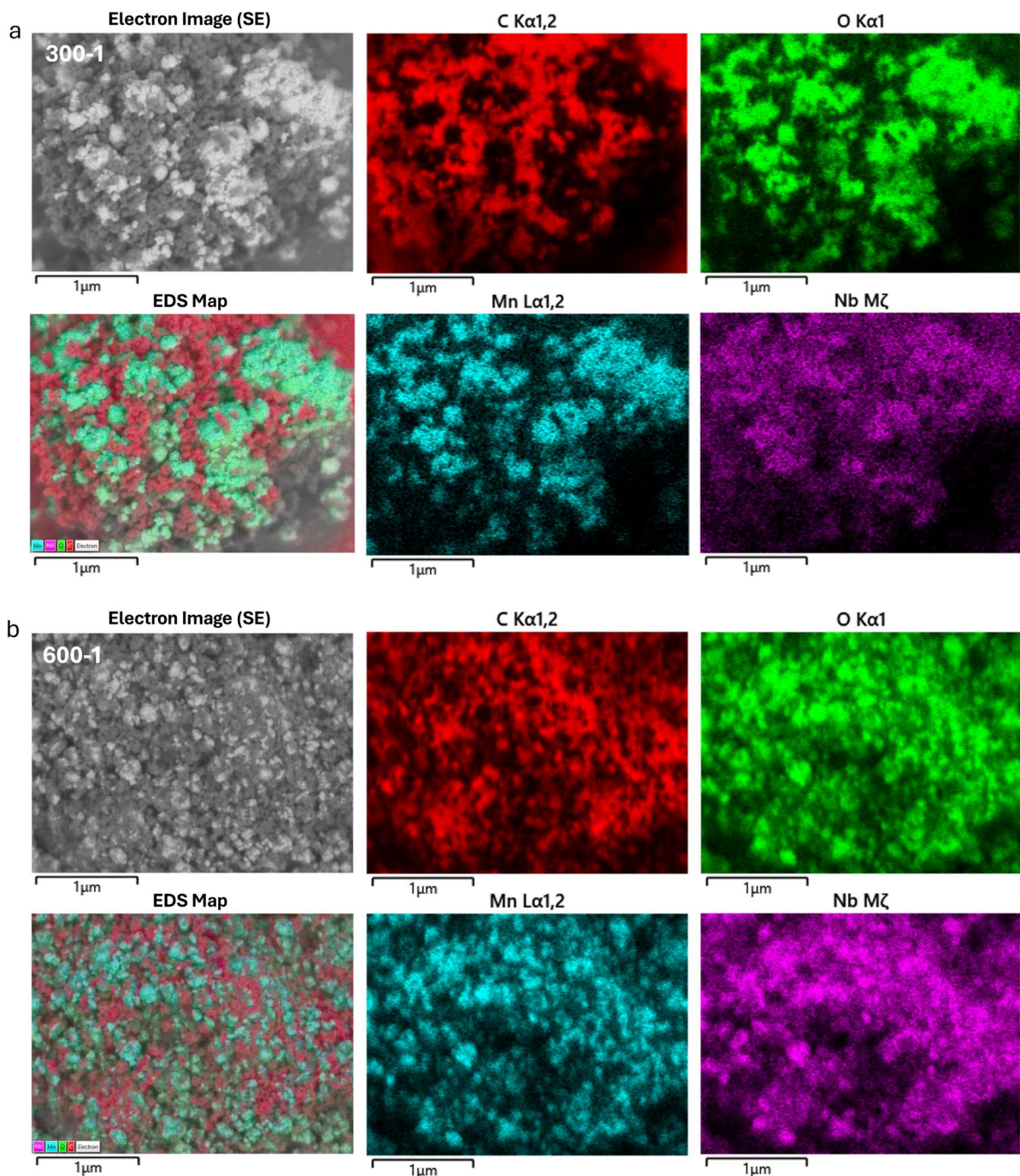


Figure S3. Energy Dispersive Spectroscopy (EDS) maps and corresponding SEM images of (a) 300-1 and (b) 600-1 CB mixed LMNO (70:20:10).

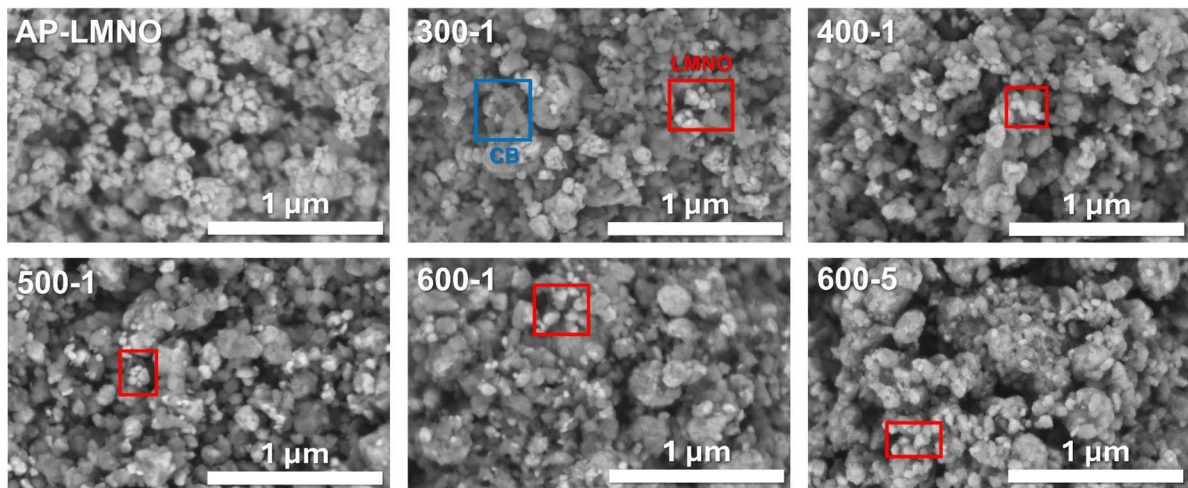


Figure S4. SEM images of AP-LMNO and CB mixed AP-LMNO samples prepared at different ball-milling RPMs and milling durations.

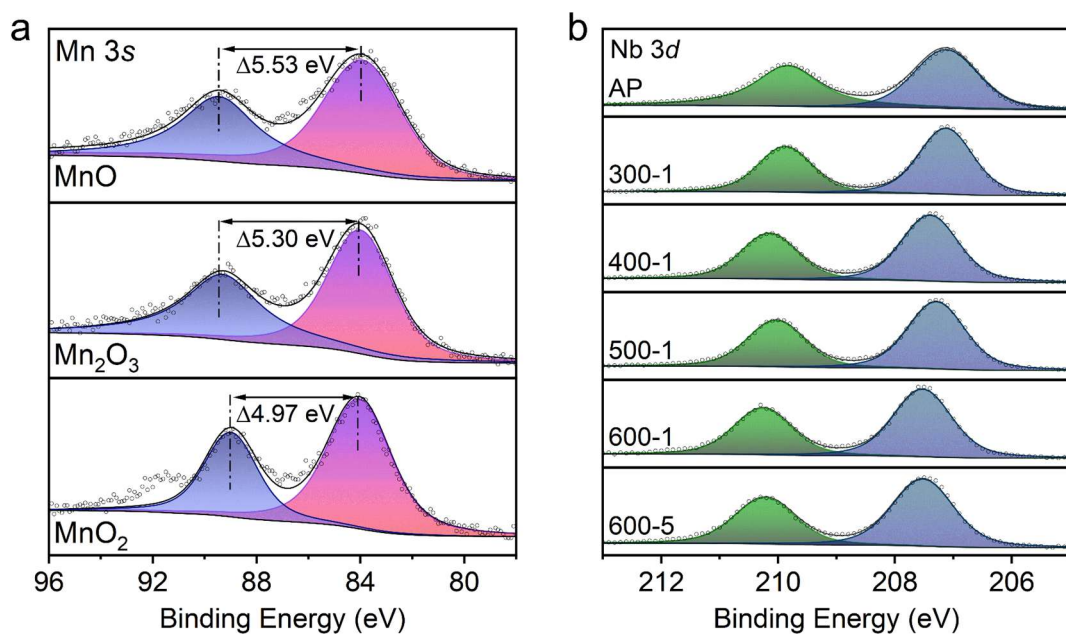


Figure S5. (a) Mn 3s XPS of various Mn oxides [MnO (Mn²⁺), Mn₂O₃ (Mn³⁺) and MnO₂ (Mn⁴⁺)]. (b) Nb 3d XPS of AP-LMNO and CB mixed LMNO.

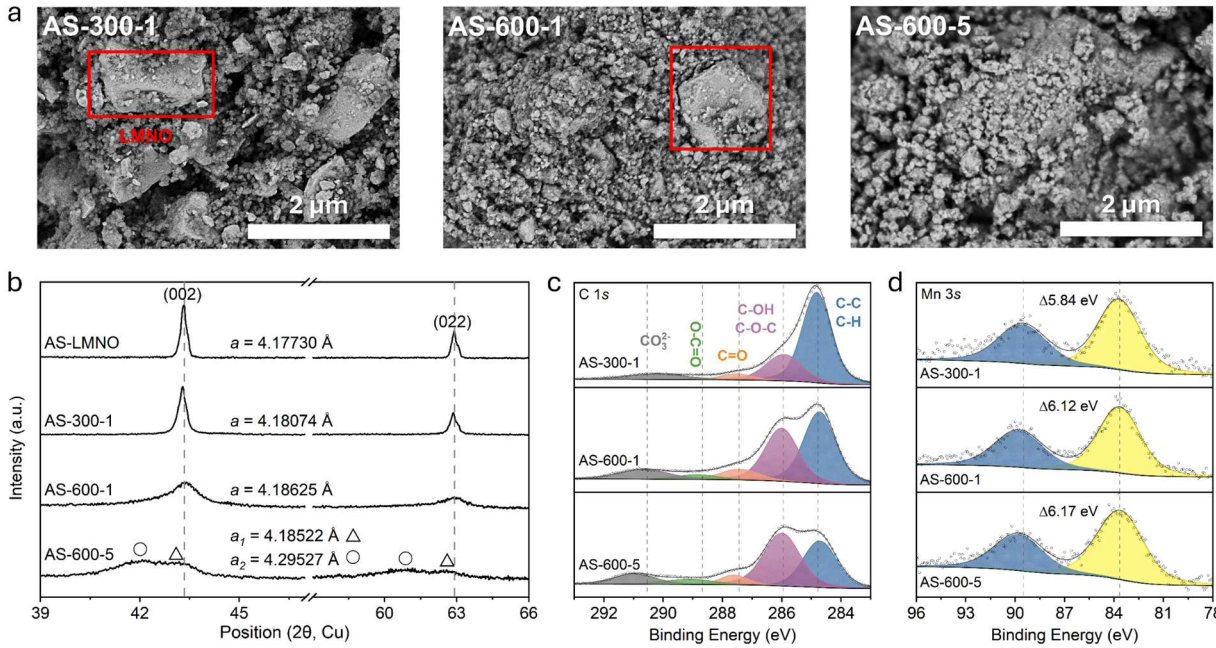
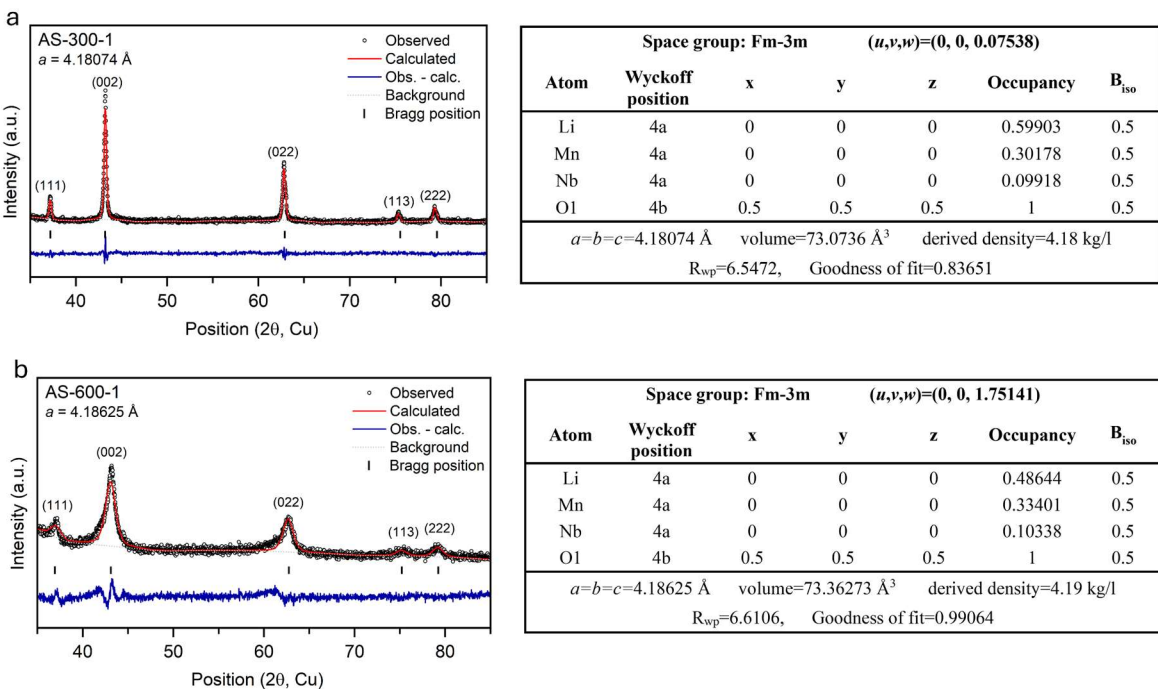


Figure S6. Milling was performed with AS-LMNO and carbon black (300 rpm for 1 h, 600 rpm for 1 h, and 600 rpm for 5 h; denoted AS-300-1, AS-600-1, and AS-600-5). (a) SEM images of AS-300-1, AS-600-1 and AS-600-5 samples. Large LMNO particles are boxed in red. (b) XRD patterns of AS-LMNO, AS-300-1, AS-600-1 and AS-600-5. (c) C 1s and (d) Mn 3s XPS spectra of AS-300-1, AS-600-1 and AS-600-5 samples charge corrected to C 1s C-C/C-H at 284.8 eV.



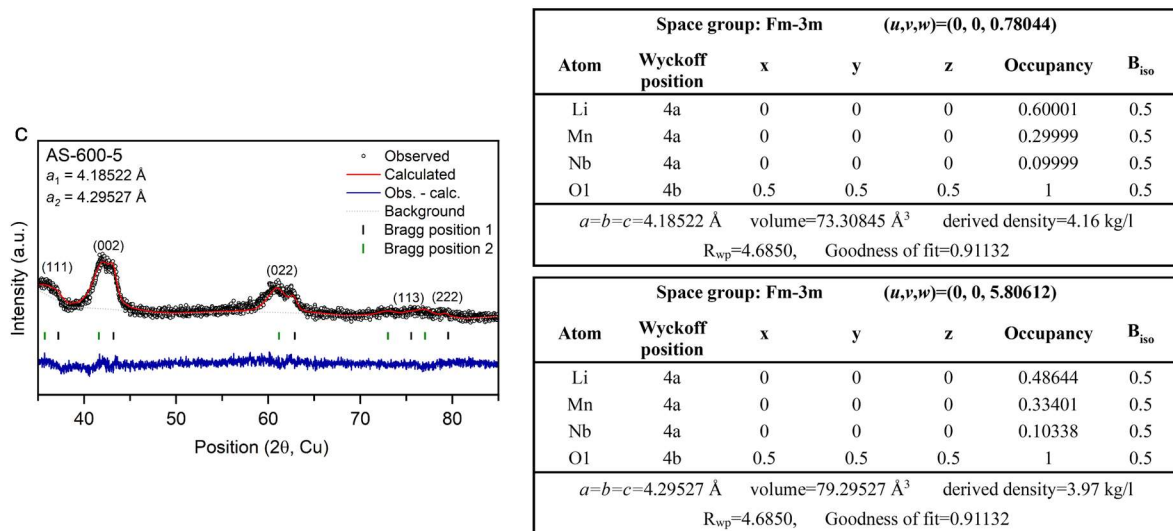


Figure S7. XRD refinement data for (a) AS-300-1, (b) AS-600-1 and (c) AS-600-5.

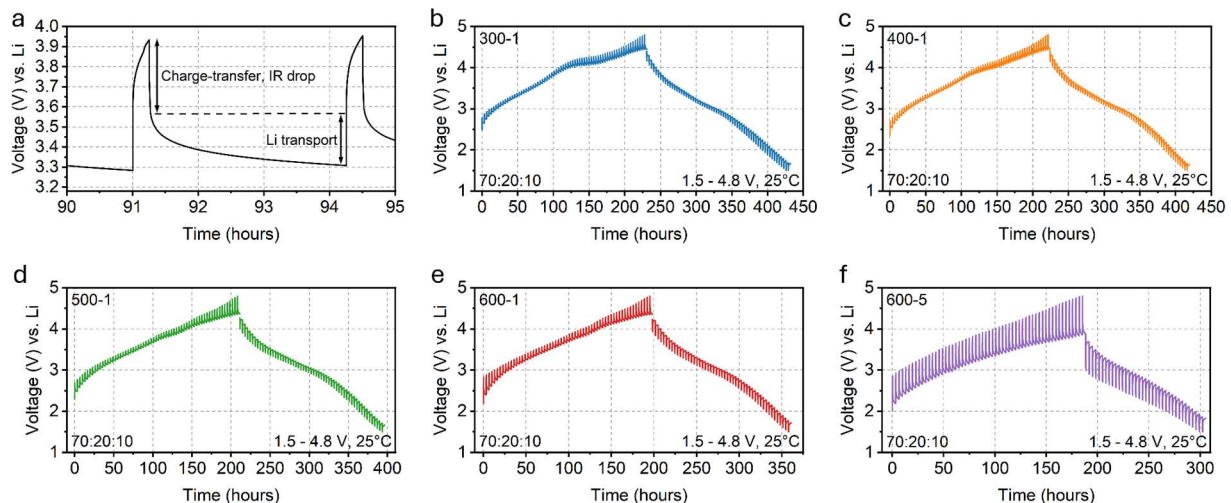


Figure S8. (a) Section of galvanostatic intermittent titration technique (GITT) highlighting the (i) initial IR drop from charge-transfer resistance followed by the (ii) time-dependent relaxation governed by mass-transport resistance. GITT measurements of (b) 300-1, (c) 400-1, (d) 500-1, (e) 600-1 and (f) 600-5 CB mixed LMNO.

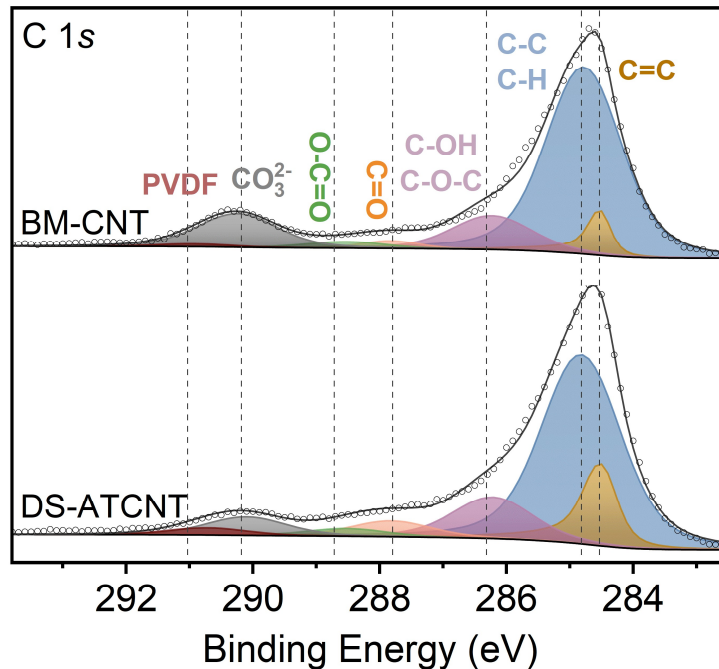


Figure S9. C 1s XPS of BM-CNT and DS-ATCNT electrodes. The electrode samples underwent argon-ion etching before XPS to remove the impurity surface layer that is formed from air exposure during electrode processing.

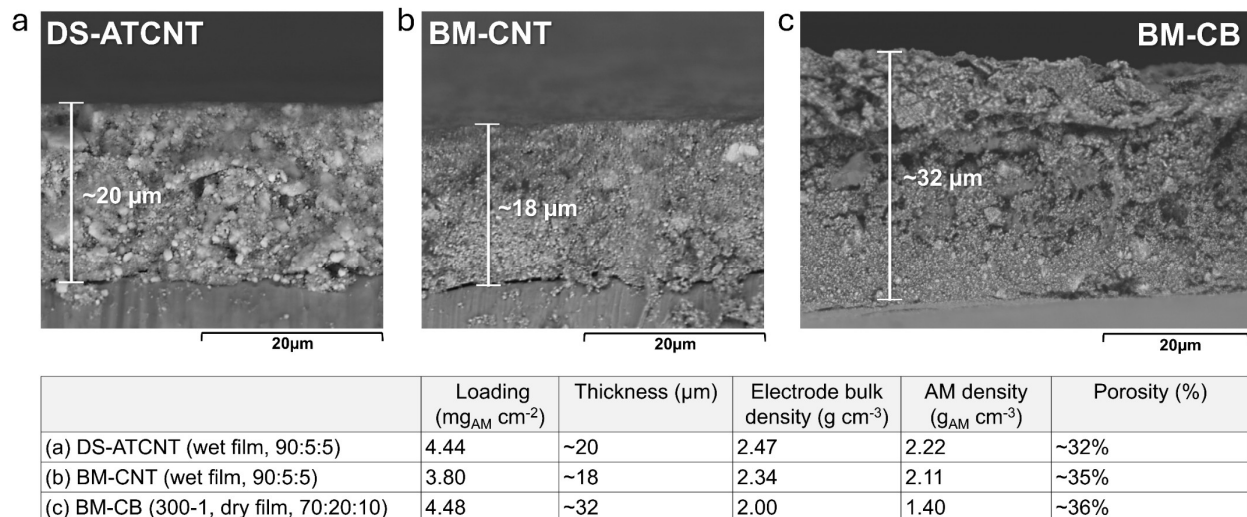


Figure S10. SEM images of electrode cross sections prepared by slicing the electrode with a precision die. (a) DS-ATCNT (wet film, 90:5:5), (b) BM-CNT (wet film, 90:5:5) and (c) BM-CB (300-1, dry film, 70:20:10) (LMNO:CNT/ATCNT/CB:PVDF/PTFE). Reported thickness values correspond to the average thickness measured across the cross section. Electrode bulk density was calculated from the total areal loading and film thickness. The effective active-material density was defined as the active-material (AM) mass per total electrode volume. Porosity was estimated from the electrode bulk density and the weighted true densities of the solid components (LMNO 4.00 g cm⁻³, PVDF 1.78 g cm⁻³, PTFE 2.20 g cm⁻³, CNTs 2.1 g cm⁻³, carbon black 2.00 g cm⁻³).

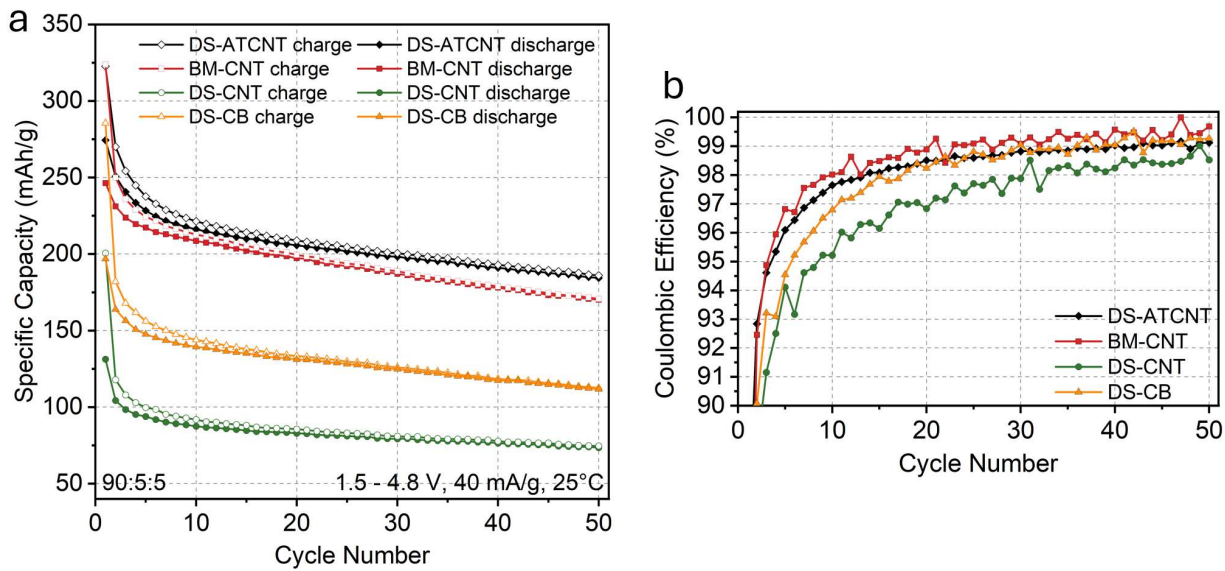
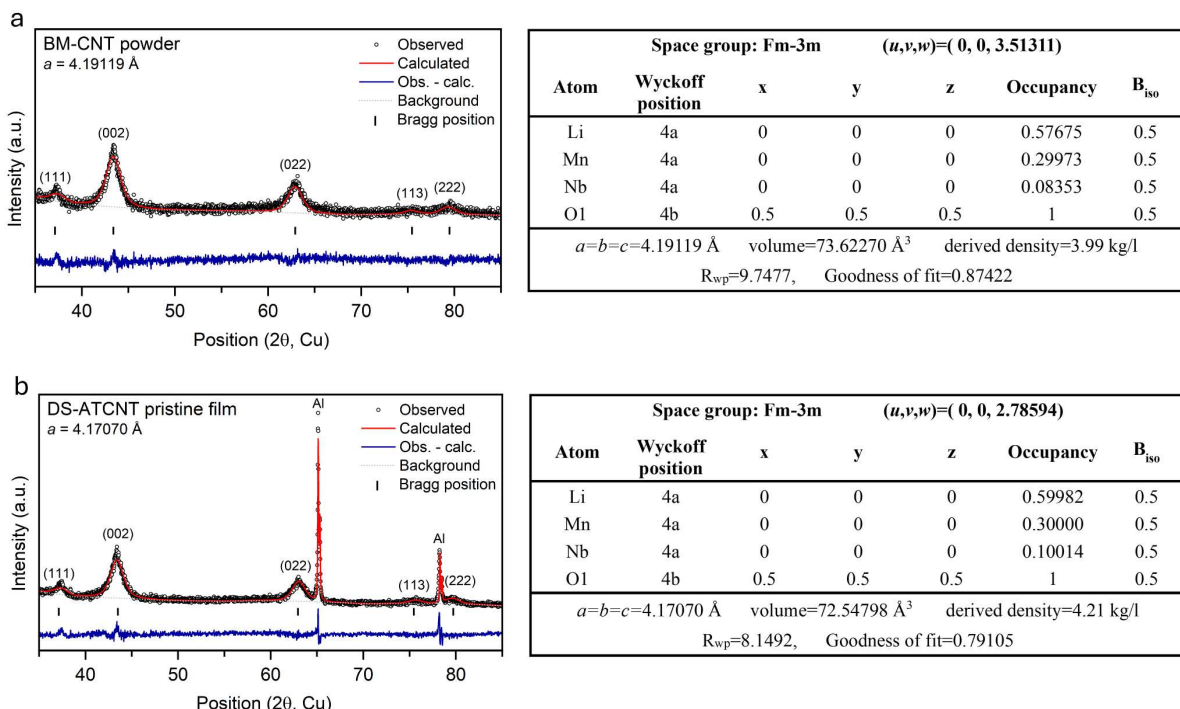


Figure S11. (a) Specific charge/discharge capacities and (b) coulombic efficiencies over 50 cycles of DS-ATCNT, BM-CNT, DS-CNT, and DS-CB cells cycled at 40 mA g^{-1} between 1.5-4.8 V.



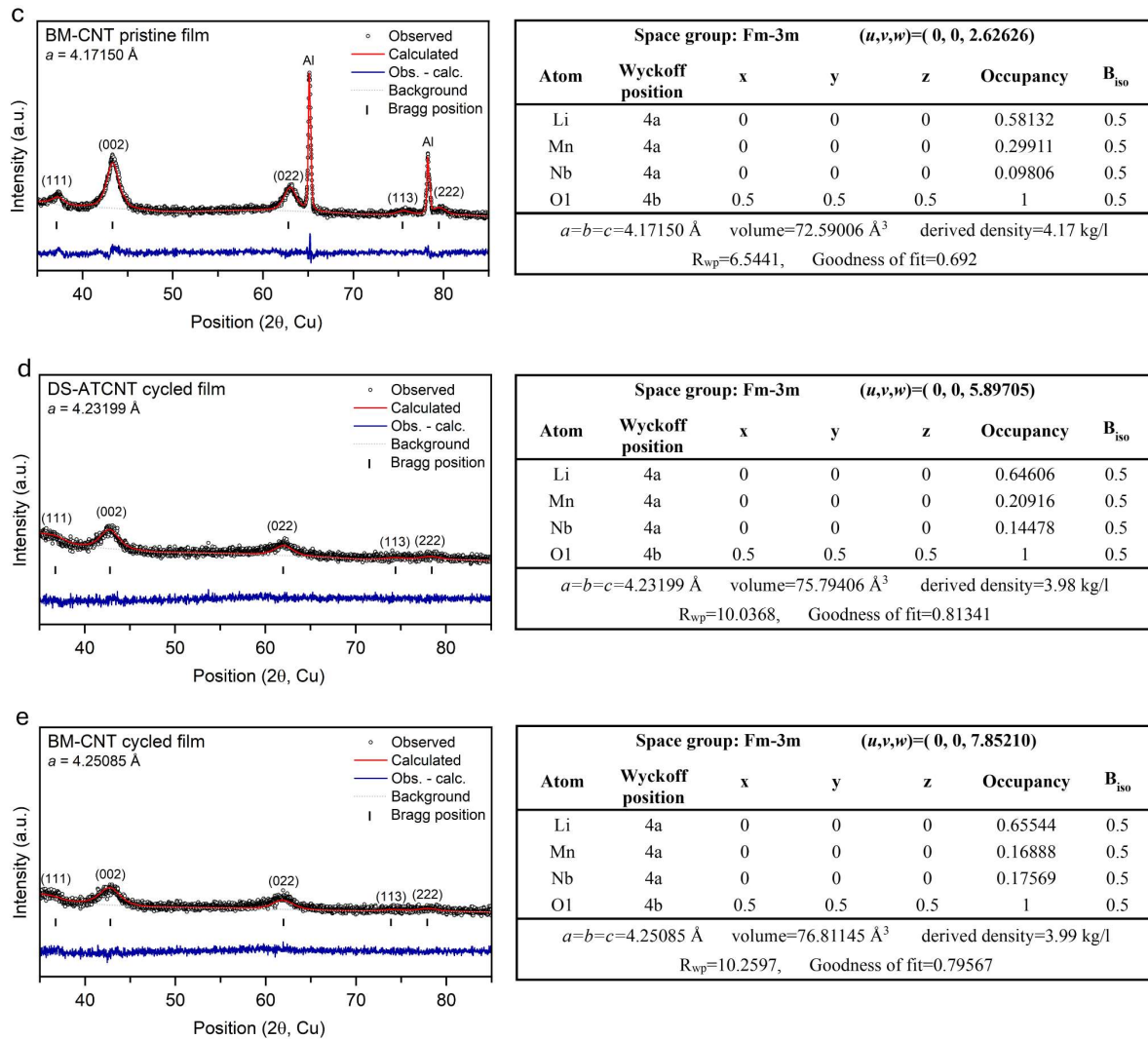


Figure S12. XRD refinement data for (a) BM-CNT powder, (b) DS-ATCNT pristine electrode, (c) BM-CNT pristine electrode, (d) DS-ATCNT electrode after 50 cycles and (e) BM-CNT electrode after 50 cycles.

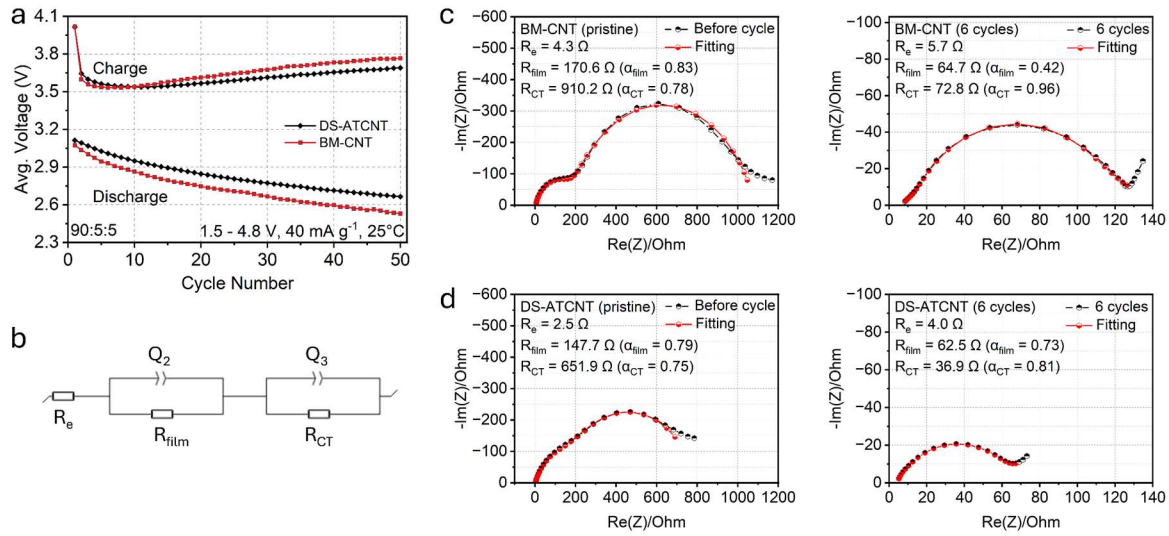


Figure S13. (a) Average charge and discharge voltages over 50 cycles between 1.5-4.8 V at 40 mA g⁻¹ for Li-metal half-cells using BM-CNT and DS-ATCNT LMNO electrodes. (b) Equivalent circuit model used to analyze the impedance response. Full electrochemical impedance spectroscopy (EIS) parameters can be found in the methods section. (c,d) Nyquist plots of Li-metal half-cells determined by EIS of (c) BM-CNT and (d) DS-ATCNT LMNO electrodes before cycling and after 6 cycles between 1.5-4.8 V at 40 mA g⁻¹.